THE JOURNAL OF PHYSICAL CHEMISTRY B

Article

pubs.acs.org/JPCB

Probing the Interactions between Ionic Liquids and Water: Experimental and Quantum Chemical Approach

Imran Khan,[†] Kiki A. Kurnia,[†] Fabrice Mutelet,[‡] Simão P. Pinho,[§,∥] and João A. P. Coutinho*[,†]

[†]Departamento de Química, CICECO, Universidade de Aveiro, Campus Universitário de Santiago, 3810-193 Aveiro, Portugal

[‡]Université de Lorraine, Ecole Nationale Supérieure des Industries Chimiques, Laboratoire Réactions et Génie des Procédés, CNRS (UMR7274), 1 rue Grandville, BP 20451 54001 Nancy, France

[§]Associate Laboratory LSRE/LCM, Departamento de Tecnologia Química e Biológica, Instituto Politécnico de Bragança, Campus de Santa Apolónia, 5301-857 Bragança, Portugal

[∥]UNIFACS-Universidade de Salvador, Rua Dr. José Peroba 251, CEP 41770-235 Salvador, Brasil

Supporting Information

ABSTRACT: For an adequate choice or design of ionic liquids, the knowledge of their interaction with other solutes and solvents is an essential feature for predicting the reactivity and selectivity of systems involving these compounds. In this work, the activity coefficient of water in several imidazolium-based ionic liquids with the common cation 1-butyl-3-methylimidazolium was measured at 298.2 K. To contribute to a deeper insight into the interaction between ionic liquids and water, COSMO-RS was used to predict the activity coefficient of water in the studied ionic liquids along with the excess enthalpies. The results showed good agreement between experimental and predicted activity coefficient of water in ionic liquids and that the interaction of water and ionic liquids was strongly influenced by the hydrogen bonding of the anion with water. Accordingly, the intensity of interaction of the anions with water can be ranked as the following: $[CF_3SO_3]^-$ < $[SCN]^-$ < $[TFA]^-$ < Br^- < $[TOS]^-$ < Cl^- < $[CH_3SO_3]^-$ $[DMP]^-$ < $[Ac]^-$. In addition, fluorination and aromatization of anions are shown to reduce their interaction with water. The effect of temperature on the activity coefficient of water at infinite dilution was measured by inverse gas chromatography and predicted by COSMO-RS. Further analysis based on COSMO-RS provided information on the nature of hydrogen bonding between water and anion as well as the possibility of anion−water complex formation.

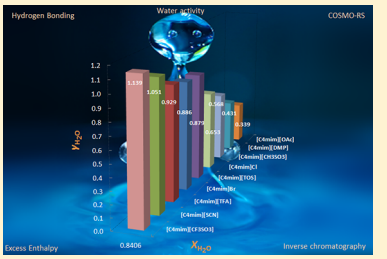

1. INTRODUCTION

Because of the hygroscopic nature of ionic liquids, their interaction with water has been most studied. Even hydrophobic ionic liquids present a high capacity to solubilize water,[1,2] and can also absorb significant amounts of water from the atmosphere.[3−6] The most widely used methods for probing the interaction of ionic liquid−water use either experimental techniques, such as infrared (IR) and nuclear magnetic resonance (NMR) spectroscopies techniques,[7−12] or theoretical calculations.[11,13−15] Cammarata et al.[7] studied the molecular state of absorbed water (0.2−1.0 mol dm^{-3}) from air in several imidazolium-based ionic liquids with various anions using attentuated total reflectance (ATR) and transmissions IR spectroscopy. They showed that the preferred sites of interaction with water molecules were the anions.[7] Their finding is further confirmed by ^{1}H NMR, molecular dynamic (MD) simulations, and density functional theory.[2,7,12,16−20] Thus, the anion plays a crucial role in the ionic liquid interaction with water. While some authors attribute that role to H-bonding, others discuss the role of electrostatic interactions occurring between molecules in the mixtures.[12,19,20] One of the main problems is the lack of energetic characteristics of ionic liquid−water interaction where one can separate H-bond and electrostatic energy in those molecules in the mixture.

Conductor-like screening model for real solvents (COSMO-RS) is arguably the simplest yet most powerful method for probing the energetic characteristics of molecular interaction between ionic liquid−solute/solvent fluids. Indeed, the molecular interaction of ionic liquids with various organic solvents has been successfully elucidated using COSMO-RS.[21−25] The advantages of COSMO-RS in comparison with other methods for the prediction of thermodynamic behavior of fluids, such as non-random two liquid (NRTL), UNIFAC, or UNIQUAC, is the fact that it does not require a large bank of experimental data. COSMO-RS is a unique method for predicting the thermodynamic behavior of compounds in the pure and mixed state on the basis of unimolecular quantum chemical calculations for the individual molecules. In addition, it has been shown to be very helpful as an a priori tool for finding suitable ionic liquid candidates for a certain task or specific applications before extensive experimental measurements.[26] Anantharaj and Banerjee applied COSMO-RS to screen potential ionic liquids for denitrification[26] and desulphurization of diesel oil.[27] Palomar and collaborators used

Received: November 19, 2013
Revised: January 20, 2014
Published: January 27, 2014

COSMO-RS to predict the Henry's law constant and the excess enthalpy for the physical absorption of CO_2[28] and various volatile organic compounds[23] as well as the solubility of cellulose and lignin[29] in ionic liquids. Our group has been using COSMO-RS for the description of liquid−liquid equilibrium in mixtures of ionic liquids with water,[30] alcohol,[31] and hydrocarbons.[32,33] A recent work[25] showed that COSMO-RS is able to correctly describe the experimental excess enthalpies and thus the molecular interactions of ionic liquids and water.

Taking into account the importance of the interaction of ionic liquid and water and the high reliability of COSMO-RS to predict the energetic interaction, this work was carried out to get a deeper understanding of the mechanisms that rule their interaction through complementary experimental and theoretical studies. This work is a continuation of our systematic investigations toward the understanding of the interaction of ionic liquids with water.[34−37] Under this scenario, a systematic measurement of the activity coefficients of water in various ionic liquids with the common cation 1-butyl-3-methylimidazolium, $[C_4mim]^+$, and a theoretical analysis of ionic liquid−water thermodynamic and energetic interactions using COSMO-RS model were carried out. The $[C_4mim]^+$ cation was adopted because this cation is the most frequently studied in the literature, while the anions were chosen to cover a wide range of hydrophobicities and to get a broad picture of the structural impact on their interaction with water. Initially, the capability of COSMO-RS to predict the experimental activity coefficients of water in imidazolium-based ionic liquids is evaluated. Furthermore, the effect of temperature on the activity coefficient of water at infinite dilution in the ionic liquids was studied by inverse gas chromatography and predicted also with COSMO-RS. In the last part of this work, the consistent information compiled relative to the water activity coefficient studies using COSMO-RS encouraged its application for the estimation of energetic effects and the identification of the most important features in water−ionic liquid interactions.

2. EXPERIMENTAL SECTION

2.1. Materials. The studied ionic liquids 1-butyl-3-methylimidazolium chloride $[C_4mim]Cl$ (99 wt %), 1-butyl-3-methylimidazolium bromide $[C_4mim]Br$ (99 wt %), 1-butyl-3-methylimidazolium acetate $[C_4mim][Ac]$ (98 wt %), 1-butyl-3-methylimidazolium trifluoroacetate $[C_4mim][TFA]$ (98 wt %), 1-butyl-3-methylimidazolium methanesulfonate $[C_4mim][CH_3SO_3]$ (99 wt %), 1-butyl-3-methylimidazolium trifluoromethanesulfonate $[C_4mim][CF_3SO_3]$ (99 wt %), 1-butyl-3-methylimidazolium tosylate $[C_4mim][TOS]$ (99 wt %), 1-butyl-3-methylimidazolium thiocyanate $[C_4mim][SCN]$ (98 wt %), and 1-butyl-3-methylimidazolium dimethylphosphate $[C_4mim][DMP]$ (98 wt %) were obtained from IoLiTec (Germany). Prior to the measurement of the activity coefficient, the individual samples of each ionic liquid were dried at moderate temperature (≈ 323 K) and at high vacuum (≈ 10^{-3} Pa), under constant stirring, and for a minimum period of 48 h to remove traces of water and volatile compounds. The purities of these ionic liquids were further checked by ^1H, ^{13}C, and ^{19}F-NMR (when appropriate) and were shown to be ≥99 wt %. The water content of each ionic liquid was determined by Karl Fischer titration (Mettler Toledo DL32 Karl Fischer coulometer using the Hydranal-Coulomat E from Riedel-de Haen as analyte) and found to be less than 30×10^{-6} mass fraction. Double-distilled water, passed through a reverse osmosis system and further treated with a Milli-Q plus 185 water purification equipment, was used in all experiments. Figure 1 depicts the chemical structures of the studied compounds.

2.2. Measurement of Water Activities and Water Activity Coefficients. The measurements of water activities (a_w) were performed using a Novasina hygrometer LabMaster-a_w (Switzerland). The measuring principle of the instrument is based on resistive-electrolytic method. The accuracy of the instrument is 0.001 a_w, enabling measurements under controlled chamber temperature conditions (±0.15 K), and was previously calibrated with six saturated pure salt standard solutions (water activities ranging from 0.113 to 0.973), which were included in the instrument. However, to achieve the given accuracy,

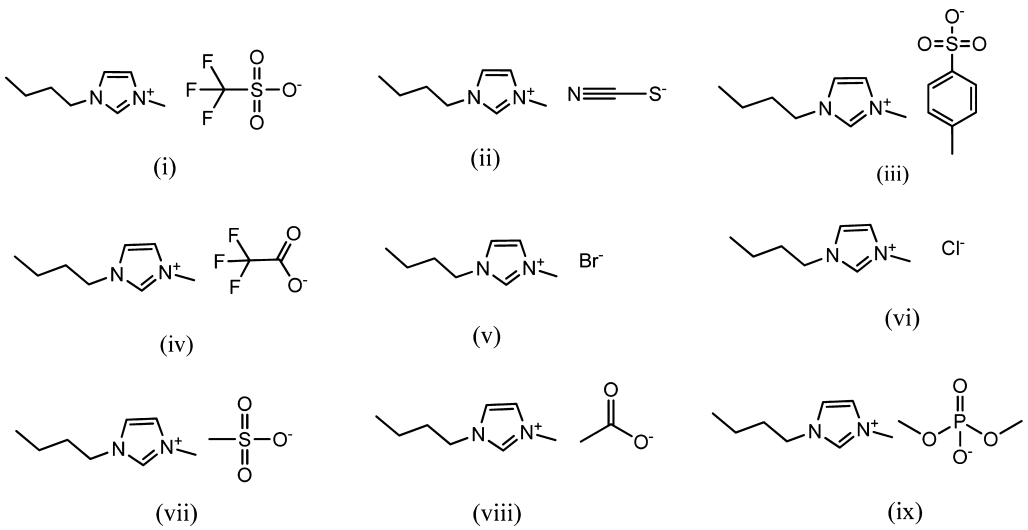

Figure 1. Chemical structures of the studied imidazolium-based ionic liquids: (i) 1-butyl-3-methylimidazolium trifluoromethanesulfonate, $[C_4mim][CF_3SO_3]$; (ii) 1-butyl-3-methylimidazolium thiocyanate, $[C_4mim][SCN]$; (iii)1-butyl-3-methylimidazolium tosylate, $[C_4mim][TOS]$; (iv)1-butyl-3-methylimidazolium trifluoroacetate, $[C_4mim][TFA]$; (v) 1-butyl-3-methylimidazolium bromide, $[C_4mim][Br]$; (vi) 1-butyl-3-methylimidazolium chloride, $[C_4mim][Cl]$; (vii) 1-butyl-3-methylimidazolium methanesulfonate, $[C_4mim][CH_3SO_3]$; (viii) 1-butyl-3-methylimidazolium acetate, $[C_4mim][Ac]$; (ix) 1-butyl-3-methylimidazolium dimethylphosphate, $[C_4mim][DMP]$.

dx.doi.org/10.1021/jp4113552 | J. Phys. Chem. B 2014, 118, 1848−1860

a calibration curve was built using either KCl or $CaCl_2$ aqueous solutions at different salt molalities, depending on the magnitude of the water activity values to be measured. The obtained values were compared to those recommended in the extensive reviews by Archer[36,38] for KCl or Rard and Clegg[39] for $CaCl_2$. For each measurement, samples of approximately 2−3 cm^3 prepared in the entire solubility range of the ILs, with a water mole fraction uncertainty of ±0.0001, were charged in the measuring dishes and placed in the airtight equilibrium chamber. The exchange of free water takes place until the partial pressure of water vapor reaches the equilibrium, which is confirmed following the a_w variation with time. When a constant value is reached, the water activity is recorded. Diluted solutions reach equilibrium in less than 1 h, but solutions with high concentration of ionic liquids could take up to 8 h. The water activity coefficient (γ_w) is then calculated from the water activities as

$$\gamma_w = \frac{a_w}{x_w} \tag{1}$$

where a_w is the water activity, and x_w is the mole fraction of water.

2.3. Measurement of Activity Coefficients at Infinite Dilution. The activity coefficient of water at infinite dilution in the ionic liquids was measured using the same method previously reported by us.[37] Inverse chromatography experiments were carried out using a Bruker (U.S.) 450-GC gas chromatograph equipped with a heated on-column injector and a thermal conductivity detector (TCD). The injector and detector temperatures were kept constant at 523 K during all experiments. To obtain adequate retention times, the helium flow rate was adjusted. Air was used to determine the column hold-up time. Exit gas flow rates were measured with a soap bubble flow meter. The temperature of the oven was determined with a Pt100 probe and controlled with an uncertainty of 0.1 K. A computer directly recorded the detector signals and the corresponding chromatograms were generated using the Galaxie Chromatography Software. Using a rotary evaporation preparatory technique, 1.0 m length columns were packed with a stationary phase, consisting of 0.20−0.35 mass fraction of IL on Chromosorb WHP (60−80 mesh) sorbent media. After the solvent (ethanol) evaporation, under vacuum, the support was left to equilibrate, at 333 K for 6 h. Prior to the measurements, each packed column was conditioned for 12 h at 363 K with a helium flow rate of 20 $cm^3\,min^{-1}$. The packing level was calculated from the masses of the packed and empty columns and was checked throughout the experiments. The weight of the stationary phase was determined with a precision of ±0.0003 g. A headspace sample volume of $(1-5) \times 10^{-3}$ cm^3 was injected to satisfy infinite dilution conditions. To confirm reproducibility, each experiment was repeated at least three times. Retention times were rigorously reproducible with an uncertainty of about 0.05−0.5 s. To verify the stability under these experimental conditions, ruling out elution of the stationary phase by the helium stream, measurements of retention time were repeated systematically each day for three solutes (octane, benzene, and ethanol). No changes in the retention times were observed during this study.

The retention data garnered by inverse chromatography experiments were used to calculate partition coefficients of water in the different ILs. The standardized retention volume, V_N, was calculated following the relationship[40,41]

$$V_N = JU_0 t'_R \frac{T_{col}}{T_{rt}}\left(1 - \frac{p^0_w(T_{rt})}{p_{out}}\right) \tag{2}$$

where the adjusted retention time, t'_R, was taken as the difference between the retention time of water and that of air; T_{col} is the column temperature, U_0 the flow rate of the carrier gas measured at room temperature (T_{rt}), $p^0_w(T_{rt})$ the vapor pressure of water at T_{rt}, and p_{out} the outlet pressure.

The factor J in eq 1 corrects for the influence of the pressure drop along the column and is given by the relation[40,41]

$$J = \frac{3}{2}\frac{\left[\left(\frac{p_{in}}{p_{out}}\right)^2 - 1\right]}{\left[\left(\frac{p_{in}}{p_{out}}\right)^3 - 1\right]} \tag{3}$$

where p_{in} is the inlet pressure.

Activity coefficients at infinite dilution of water in each IL, γ^∞_w, were calculated by[40,41]

$$\ln(\gamma^\infty_w) = \ln\left(\frac{n_2 RT}{V_N p^0_w(T)}\right) - p^0_w(T)\left(\frac{B_{ww} - V^0_w}{RT}\right) + \left(\frac{2B_{w3} - V^\infty_w}{RT}\right)Jp_{out} \tag{4}$$

where n_2 is the number of moles of stationary phase component within the column, R the ideal gas constant, T the oven temperature, B_{ww} the second virial coefficient of the solute in the vapor state at temperature T, B_{w3} the mutual virial coefficient between water and the carrier gas (helium, denoted by "3"), and $p^0_w(T)$ the probe's vapor pressure at temperature T. The values of p^0_w result from correlated experimental data. The molar volume of the water at temperature T, V^0_w, was determined from experimental densities, and the partial molar volumes of the water at infinite dilution, V^∞_w, were assumed to be equal to V^0_w. The data required for the calculation of these parameters were taken from previous works.[42] The uncertainties in activity coefficient at infinite dilution γ^∞_w were estimated to be less than 3% based on error propagation analyses, which took into consideration uncertainties in the following experimental quantities and their standard deviations given in parentheses after the quantity: inlet and outlet pressures (0.2 kPa); adjusted retention time of the solute, t_R' (0.01 min); mass of the stationary phase (2%); flow rate of the helium carrier gas (0.1 $cm^3\,min^{-1}$); and oven temperature (0.2 K).

2.4. COSMO-RS. COSMO-RS is a novel and fast methodology for predicting thermochemical properties of fluids in their pure and mixture state based on unimolecular quantum chemical calculations. The detail theory of COSMO-RS can be found in the original work of Klamt.[43] Only the major features for understanding the analysis and discussion in the present work are highlighted here. The first step in the COSMO-RS prediction procedure is applying the continuum solvation model COSMO to simulate a virtual conductor environment for the molecule of interest. This is then followed by a screening charge density σ_i, on the nearby conductor, obtained through the standard quantum chemical calculation. The 3D distribution of the screening charge density on the surface of each molecule is converted into a surface composition function, called the sigma profile (σ-profile), $p(\sigma)$. In the second step, the statistical thermodynamics treatment of the molecular interactions is performed in the COSMOtherm software using the parameter file BP_TZVP_C30_1301 (COSMOlogic GmbH & Co KG,

dx.doi.org/10.1021/jp4113552 | J. Phys. Chem. B 2014, 118, 1848−1860

Leverkusen, Germany).[44] The interaction energies of the surface pairs are defined in terms of the screening charge densities σ and σ' of the respective surface segments. Subsequently, the chemical potential (μ_s) of a surface segment (σ), the so-called sigma potential (σ-potential), is calculated using the following equation:

$$\mu_s(\sigma) = -\frac{RT}{a_{eff}} \ln\left[\int p_s(\sigma') \exp\left\{\frac{a_{eff}}{RT}[\mu_s(\sigma') - E_{misfit}(\sigma, \sigma') - E_{HB}(\sigma, \sigma')]\right\} d\sigma'\right] \quad (5)$$

where a_{eff} represents the effective contact area and $p_s(\sigma)$ stands for the surface screening charge distribution of the whole system. The chemical potential of a compound is available from the integration of the σ-potential over the surface of the molecule. The capability of COSMO-RS to calculate the chemical potential of an arbitrary solute x in any pure or mixed solvent S at variable temperature enables the prediction of thermodynamic properties such as activity coefficient of water in the ionic liquids.

For the study involving ionic liquids, the complete dissociation into cation and anion was assumed. The charge distribution of screening charge densities, displayed as σ-profile of the ionic liquid, is simply determined as the sum of the σ-profile of the cation and anion

$$p_{ionic\ liquid}(\sigma) = p_{cation}(\sigma) + p_{anion}(\sigma) \quad (6)$$

where $p_{cation}(\sigma)$ and $p_{anion}(\sigma)$ are the sigma profiles for the cation and anion, respectively. This was equivalent to calculating the sigma profile of a mixture consisting of the cation and anion.

The COSMO files of the molecules considered in this work were taken from the database of COSMOtherm software (COSMOlogic GmbH & Co KG, Leverkusen, Germany), in which the molecular geometry of water and each ion were optimized by utilizing BP functional B88-P86 with a triple-ζ valence polarized basis set (TZVP) and the resolution of identity standard (RI) approximation.[44] The details of the calculation and procedure of estimating activity coefficient using COSMO-RS can be found elsewhere,[45,46] and the procedure of estimating excess enthalpy can be found in our recent work.[25]

The excess enthalpies of interaction between water and ionic liquids are calculated using the following equation:[22]

$$H^E = H_{i,mixture} - H_{i,pure} \quad (7)$$

To understand the contribution of specific interaction from each species to the total excess enthalpy (H^E), the following equation was considered:

$$H^E = H^E cation + H^E anion + H^E water \quad (8)$$

The H^E in the COSMO-RS method arises from summing the three specific interactions, namely electrostatic misfit H^E_{MF}, hydrogen bonds H^E_{HB}, and van der Waals forces H^E_{vdW}. Thus, eq 8 can be written as the contribution of three specific interactions according to eqs 9 to 11.

$$H^E cation = H^E_{MF} cation + H^E_{HB} cation + H^E_{vdW} cation \quad (9)$$

$$H^E anion = H^E_{MF} anion + H^E_{HB} anion + H^E_{vdW} anion \quad (10)$$

$$H^E water = H^E_{MF} water + H^E_{HB} water + H^E_{vdW} water \quad (11)$$

Therefore, COSMO-RS allows the determination of the energetic contribution of three specific interactions of each species in the mixture to the total excess enthalpy.

3. RESULTS AND DISCUSSIONS

3.1. Water Activity and Activity Coefficient in Ionic Liquids. Table 1 presents the water activities measured at 298.2 K, the experimental and predicted activity coefficient of water in each ionic liquid using COSMO-RS, and the deviations obtained by eq S1 of Supporting Information. These results indicate that water has weak interactions with [C_4mim]-[CF_3SO_3] and [C_4mim][SCN] because these ILs present water activity coefficients larger than unity (positive deviation to the ideality) in a wide range of concentrations, indicating that the water−IL interactions are unfavorable. The other ionic liquids all present negative deviations to the ideality, with the following sequence of increasing interactions with water:

$$[C_4mim][TFA] < [C_4mim]Br \sim [C_4mim][TOS] < [C_4mim]Cl < [C_4mim][CH_3SO_3] < [C_4mim][DMP] < [C_4mim][Ac]$$

This trend is in close agreement with the infinite dilution activity coefficients of water on these ionic liquids reported in Table S1 in Supporting Information. Figures 2−4, where the symbol and line represent experimental and predicted values, respectively, allow the discussion of the impact of structural variation of ionic liquids on the activity coefficient of water.

The activity coefficient of water in the two halides containing ionic liquids both present negative deviations to ideality with a monotonic behavior of increasing nonideality with the IL concentration, as depicted in Figure 2. Water has a stronger interaction, indicated by the low activity coefficient, with [C_4mim]Cl being lower than with [C_4mim]Br. The increase in size and respective decrease in charge density of the bromide in comparison with the chloride results in a weaker interaction of the [C_4mim]Br with water. COSMO-RS adequately predicts the activity coefficient of water in these two ionic liquids as a function of concentration of water in the mixture with an average absolute deviation (AAD) of 6.9 and 7.4% for [C_4mim]Cl and [C_4mim]Br, respectively.

The impact of the fluorination on the water activity coefficients can be gauged from the results of the [C_4mim]-[TFA] versus [C_4mim][Ac] reported in Figure 3 and [C_4mim][CH_3SO_3] versus [C_4mim][CF_3SO_3] depicted in Figure 4. In both cases the fluorination of the anion decreases the strength of the interaction between the water and the ionic liquid as shown by the increase in the activity coefficient of water upon fluorination of the anion. Like the activity coefficient of water in halide-based ionic liquids, the activity coefficient of water in [C_4mim][Ac] is also monotonic, decreasing with the increasing concentration of IL. However, a different behavior is shown by [C_4mim][CF_3SO_3], with water activity coefficients attaining a maximum around 0.75 water mole fraction, as given in Figure 4. While good quantitative predictions are observed for the activity coefficient of water in [C_4mim][Ac] (AAD = 5.6%), COSMO-RS shows itself to be capable of describing the effect of fluorination of the anion to produce distinctively higher activity coefficients but fails to describe the nonmonotonic behavior of [C_4mim][TFA], particularly for the high ionic liquid concentration solutions, resulting in higher deviation for the water activity coefficients in this IL (AAD = 10.4%).

dx.doi.org/10.1021/jp4113552 | J. Phys. Chem. B 2014, 118, 1848−1860

Table 1. Experimental and Predicted Activity Coefficient of Water in Ionic Liquids Using COSMO-RS at 298.2 K

x_w	a_w	γ_w^{exp}	$\gamma_w^{COSMO\text{-}RS}$	ARD (%)
		H_2O + $[C_4mim][CF_3SO_3]$		
0.9925	0.980	0.987	0.999	1.2
0.9840	0.976	0.992	0.996	0.4
0.9737	0.974	1.000	0.992	0.8
0.9601	0.972	1.012	0.988	2.4
0.9407	0.970	1.031	0.986	4.4
0.9164	0.963	1.051	0.989	5.9
0.8707	0.951	1.092	1.006	7.9
0.7988	0.910	1.139	1.052	7.6
0.6501	0.768	1.181	1.180	0.1
0.4059	0.455	1.121	1.443	28.7
0.3389	0.378	1.115	1.527	37.0
0.1803	0.198	1.098	1.754	59.7
			AAD	13.0
		H_2O + $[C_4mim][SCN]$		
0.9897	0.977	0.987	0.998	1.1
0.9777	0.973	0.995	0.995	0.0
0.9623	0.968	1.006	0.991	1.5
0.9427	0.959	1.017	0.989	2.8
0.9161	0.950	1.037	0.994	4.1
0.8796	0.921	1.047	1.007	3.8
0.8274	0.870	1.051	1.033	1.7
0.7812	0.806	1.032	1.058	2.5
0.7346	0.701	0.954	1.082	13.4
0.5598	0.414	0.740	1.151	55.5
0.3513	0.198	0.564	1.191	111.2
0.3223	0.173	0.537	1.189	121.4
			AAD	26.5
		H_2O + $[C_4mim][TFA]$		
0.9919	0.979	0.987	0.998	1.1
0.9824	0.972	0.989	0.995	0.5
0.9702	0.960	0.989	0.989	0.0
0.9538	0.942	0.988	0.983	0.5
0.9335	0.926	0.992	0.976	1.7
0.9047	0.886	0.979	0.966	1.4
0.8606	0.813	0.945	0.947	0.2
0.7812	0.654	0.837	0.897	7.2
0.7784	0.646	0.830	0.895	7.8
0.6135	0.355	0.579	0.764	24.3
0.6061	0.343	0.566	0.759	25.4
0.5534	0.291	0.526	0.719	25.4
			AAD	7.9
		H_2O + $[C_4mim]Br$		
0.9908	0.980	0.989	0.996	0.7
0.9796	0.972	0.992	0.985	0.7
0.9652	0.954	0.988	0.963	2.5
0.9480	0.931	0.982	0.931	5.2
0.9229	0.892	0.967	0.883	8.7
0.8897	0.827	0.929	0.821	11.6
0.8406	0.745	0.886	0.740	16.5
0.7566	0.572	0.756	0.639	15.5
0.5898	0.297	0.504	0.530	5.2
0.5064	0.215	0.425	0.498	18.6
			AAD	8.4
		H_2O + $[C_4mim][TOS]$		
0.9936	0.985	0.991	0.998	0.7
0.9856	0.981	0.995	0.993	0.2
0.9756	0.976	1.000	0.985	1.5
0.9631	0.961	0.998	0.974	2.4
0.9446	0.948	1.004	0.958	4.6
0.9194	0.904	0.983	0.933	5.1
0.8749	0.844	0.965	0.886	8.2
0.8156	0.717	0.879	0.823	6.4
0.6658	0.440	0.660	0.701	6.7
0.5891	0.334	0.567	0.658	16.0
			AAD	5.2
		H_2O + $[C_4mim]Cl$		
0.9980	1.000	1.002	1.000	0.2
0.9894	0.994	1.005	0.995	1.0
0.9815	0.972	0.990	0.986	0.4
0.9677	0.945	0.976	0.964	1.2
0.9537	0.917	0.961	0.936	2.6
0.9403	0.885	0.941	0.906	3.7
0.9190	0.839	0.913	0.856	6.2
0.9037	0.804	0.890	0.819	8.0
0.8872	0.761	0.858	0.777	9.4
0.8661	0.700	0.808	0.726	10.1
0.8207	0.585	0.713	0.624	12.5
0.7923	0.517	0.653	0.567	13.2
0.8301	0.613	0.738	0.644	12.7
0.7607	0.445	0.585	0.513	12.3
0.6908	0.306	0.443	0.418	5.6
0.6498	0.244	0.376	0.376	0.0
0.6280	0.201	0.320	0.356	11.3
			AAD	6.1
		H_2O + $[C_4mim][CH_3SO_3]$		
0.9912	0.975	0.984	0.996	1.2
0.9808	0.965	0.984	0.985	0.1
0.9630	0.927	0.963	0.955	0.8
0.9513	0.904	0.950	0.932	1.9
0.9307	0.847	0.910	0.889	2.3
0.8975	0.754	0.840	0.817	2.7
0.8497	0.625	0.736	0.720	2.2
0.7674	0.436	0.568	0.589	3.7
0.6236	0.235	0.377	0.450	19.4
0.5881	0.191	0.325	0.429	32.0
			AAD	6.6
		H_2O + $[C_4mim][DMP]$		
0.9923	0.976	0.984	0.999	1.6
0.9832	0.965	0.981	0.994	1.3
0.9604	0.924	0.962	0.970	0.8
0.9479	0.889	0.938	0.952	1.5
0.9100	0.798	0.877	0.872	0.6
0.8871	0.718	0.809	0.814	0.6
0.8704	0.651	0.748	0.768	2.7
0.8411	0.564	0.671	0.689	2.8
0.7891	0.456	0.578	0.555	4.0
0.7612	0.381	0.501	0.492	1.7
0.6926	0.282	0.407	0.368	9.6
0.6206	0.182	0.293	0.275	6.2
			AAD	2.8
		H_2O + $[C_4mim][Ac]$		
0.9897	0.971	0.981	0.996	1.5
0.9778	0.956	0.978	0.985	0.7
0.9651	0.923	0.956	0.969	1.4
0.9425	0.862	0.915	0.935	2.2
0.9176	0.784	0.854	0.889	4.1
0.8813	0.652	0.740	0.806	8.9
0.8317	0.512	0.616	0.672	9.1
0.7428	0.309	0.416	0.438	5.3
0.7220	0.245	0.339	0.392	17.4
			AAD	5.6

dx.doi.org/10.1021/jp4113552 | J. Phys. Chem. B 2014, 118, 1848−1860

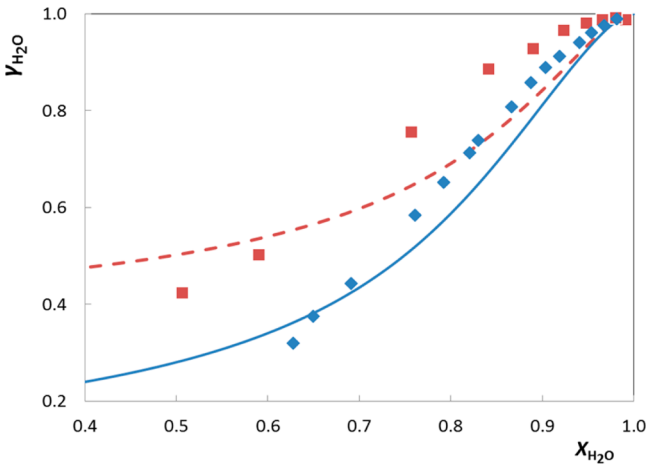

Figure 2. Experimental and predicted activity coefficient of water in ionic liquids using COSMO-RS at 298.2 K. Symbols: (♦, solid line), [C_4mim]Cl; (■, dashed line), [C_4mim]Br.

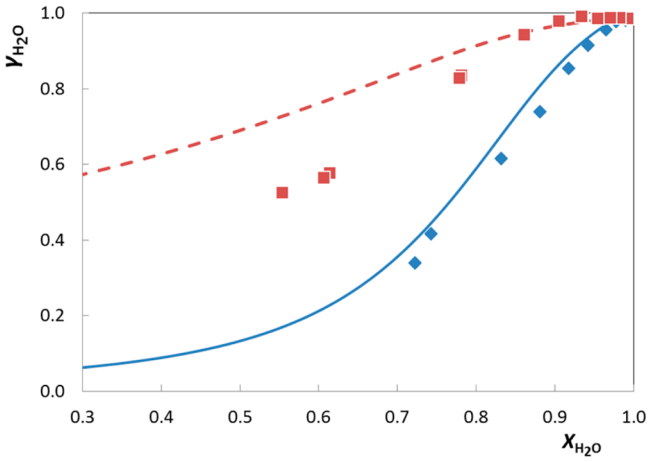

Figure 3. Experimental and predicted activity coefficient of water in ionic liquids predicted using COSMO-RS at 298.2 K. Symbols: (♦, solid line), [C_4mim][Ac]; (■, dashed line), [C_4mim][TFA].

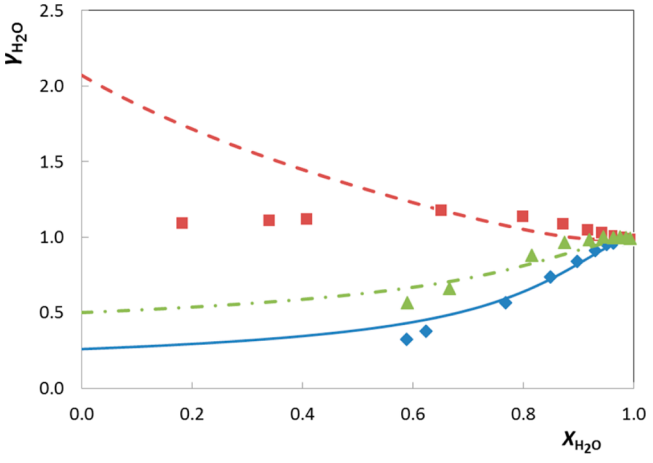

Figure 4. Experimental and predicted activity coefficient of water in ionic liquids predicted using COSMO-RS at 298.2 K. Symbols: (♦, solid line), [C_4mim][CH_3SO_3]; (■, dashed line), [C_4mim][CF_3SO_3]; (▲, dashed and dotted line), [C_4mim][TOS].

Figure 4 also allows the study of the effect of substituting $-CH_3$ in [C_4mim][CH_3SO_3] with an aromatic ring, as in the case of [C_4mim][TOS]. The results show that the phenyl group also decreases the interaction with the water as expressed in the increase in the water activity coefficient when compared to that of [C_4mim][CH_3SO_3]. Despite the COSMO-RS failure to correctly predict the activity coefficient of water in [C_4mim][CF_3SO_3], it is able to correctly predict the trend of structural variation on the activity coefficient of water in these particular sulfonate-based ionic liquids. In fact, COSMO-RS could produce quantitative predictions for the activity coefficient of water in [C_4mim][CH_3SO_3] (AAD = 6.6%) and [C_4mim]-[TOS] (AAD = 5.2%).

The two other systems studied [C_4mim][DMP] presents a monotonic behavior, similar to most systems reported here, and together with [C_4mim][Ac] are the most hydrophilic compounds with the lowest activity coefficients and thus strongest interactions with water. In contrast, the activity coefficients of water in [C_4mim][SCN] show a maximum around x_{H_2O} = 0.8, and along with [C_4mim][CF_3SO_3] these are the studied ILs presenting the weakest interactions with water. Figure 5 shows

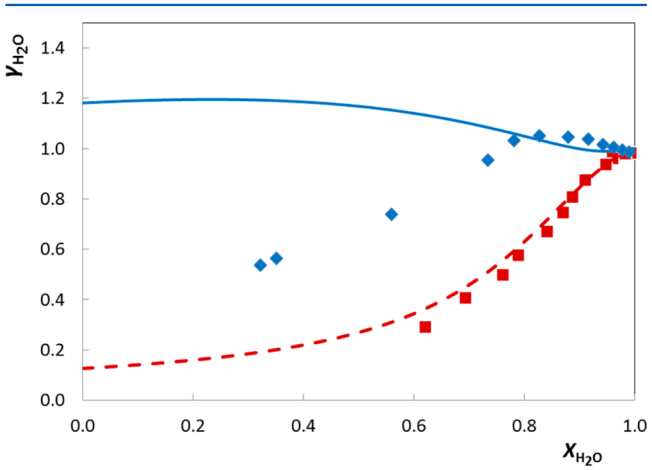

Figure 5. Experimental and predicted activity coefficient of water in ionic liquids predicted using COSMO-RS at 298.2 K. Symbols: (♦, solid line), [C_4mim][SCN]; (■, dashed line), [C_4mim][DMP].

the experimental and COSMO-RS-predicted activity coefficient of water in ionic liquids for [C4mim][SCN] and [C4mim]-[DMP] where the predictions of COSMO-RS, while qualitatively correct and identifying a positive deviation to ideality on the [C_4mim][SCN] system and the high hydrophilicity of the [C_4mim][DMP], fails to provide a good quantitative description of the activity coefficient of water in the former ionic liquid.

3.2. Infinite Dilution Activity Coefficient of Water in Ionic Liquids. The experimental activity coefficients of water at infinite dilution γ_w^∞ in ionic liquids and the predictions using COSMO-RS are given in Table S1 in Supporting Information. Unlike the activity coefficients derived from water activities that covered a wide concentration range but were measured at a single temperature, the γ_w^∞ values are available in the temperature range of 328−393 K. Two types of temperature dependency are observed for γ^∞. As shown in Figure 6, most systems present γ^∞ values that increase with temperature, indicating that the interaction between water and the ionic liquid becomes less favorable. However, for the ionic liquid [C_4mim][CF_3SO_3], the increment of temperature resulted in a decrease of γ_w^∞, i.e., in a more favorable interaction of water

dx.doi.org/10.1021/jp4113552 | J. Phys. Chem. B 2014, 118, 1848−1860

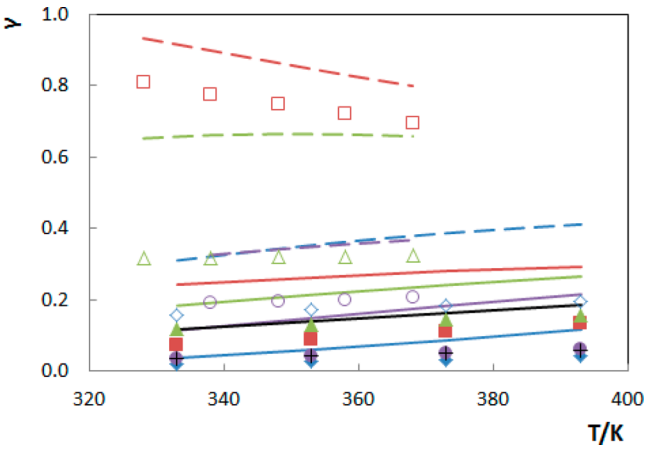

Figure 6. Experimental activity coefficient of water in ionic liquids at infinite dilution as function of temperature. Symbols: (◆, solid line), [C_4mim][Ac]; (●, solid line) [C_4mim][DMP]; (+, solid line) [C_4mim]Cl; (■, solid line) [C_4mim]Br; (▲, solid line), [C_4mim][CH_3SO_3]; (◇, dashed line), [C_4mim][TFA]; (○, dashed line) [C_4mim][TOS] (△, dashed line), [C_4mim][SCN];[47] and (□, dashed line), [C_4mim][CF_3SO_3].[48] The symbol and colored line represents experimental and COSMO-RS prediction using independent counter ion model, respectively.

with the ionic liquid. Accordingly, the ionic liquid can be ranked according to their γ_w^∞ as follows: [C_4mim][CF_3SO_3] < [C_4mim][SCN] < [C_4mim][TOS] < [C_4mim][TFA] < [C_4mim][CH_3SO_3] < [C_4mim]Br < [C_4mim]Cl < [C_4mim][DMP] < [C_4mim][Ac].

The information given in Table S1 in Supporting Information shows the big difficulty of COSMO-RS in predicting quantitatively the water activity coefficient at infinite dilution. In all systems, those values are overestimated, with particularly high deviations for those containing [C_4mim]Br or [C_4mim][DMP]. That is not surprising because it was already observed (see Table 1) that for water mole factions lower than about 0.60, the deviations of the predicted activity coefficients generally show a big increase. In spite of that, two features must be emphasized: (i) the model correctly predicts the variation of the water activity coefficient at infinite dilution with the temperature and (ii) the relative magnitude of those coefficients, between all the systems, is in very good agreement when ranking ILs by the experimental and predicted values.

From the temperature dependence of the water activity coefficient at infinite dilution, the partial molar excess enthalpies of water at infinite dilution $\bar{H}_w^{E,\infty}$ were calculated according to

$$\frac{\partial \ln \gamma_w^\infty}{\partial(1/T)} = \frac{\bar{H}_w^{E,\infty}}{R} \quad (12)$$

The calculated $\bar{H}_w^{E,\infty}$ are given in Table 2. Except [C_4mim][CF_3SO_3], the studied systems displayed negative $\bar{H}_w^{E,\infty}$, and accordingly, the ionic liquids can be ranked based on their increasing interaction with water as the following: [C_4mim][CF_3SO_3] < [C_4mim][SCN] < [C_4mim][TOS] < [C_4mim][TFA] < [C_4mim][CH_3SO_3] < [C_4mim]Cl < [C_4mim][DMP] < [C_4mim]Br < [C_4mim][Ac] . Excepting [C_4mim]Br, the model was capable of predicting the ionic liquid rank as observed from the experimental data. This might result from some particular behavior of this ionic liquid that is not yet fully understood.

As already mentioned, (H_2O + [C_4mim][CF_3SO_3]) shows positive $\bar{H}_w^{E,\infty}$. The positive $\bar{H}_w^{E,\infty}$ was also reported for [CF_3SO_3]-based ionic liquids, namely 1-butyl-1-methylpyrrolidinium trifluoromethanesulfonate [C_4C_1pyrr][CF_3SO_3][49] and 1-butyl-3-methylpyridinium trifluoromethanesulfonate [$C_4(3)C_1$py]-[CF_3SO_3].[50] It supports the fact that the anion plays a crucial role in the interaction of water and ionic liquids regardless of the cation. The positive $\bar{H}_w^{E,\infty}$ of (H_2O + [C_4mim][CF_3SO_3]) indicates that the new established hydrogen bonding between water−[CF_3SO_3]$^-$ is energetically weak and could not overcome the loss of H_2O−H_2O hydrogen bonds upon mixing. To regain the lost hydrogen bonding network, the water molecules tend to use the energy of the system to orient themselves;[51] thus, the process becomes endothermic and entropically driven. Such phenomena have also been observed for the solubility of [Tf_2N]$^-$-based ionic liquids reported by our group.[52] This endothermicity becomes more favorable with increasing temperature, as more energy is supplied at higher temperature.

Despite the greater difficulty of COSMO-RS in predicting the activity coefficient of water in the less hydrophilic ionic liquids such as [C_4mim][CF_3SO_3] and [C_4mim][SCN], this work shows that COSMO-RS give reliable predictions of the activity coefficient of water in the other studied ionic liquids. It is also able to predict the impact of structural variation of the anion into the water activity coefficient. Therefore, COSMO-RS will now be used as a tool to further characterize the interactions between the water and the ionic liquids.

Table 2. Experimental and Estimated Partial Molar Excess Enthalpies at Infinite Dilution of Water in the Ionic Liquids

ionic liquids	$\bar{H}_{w,exp}^{E,\infty}$ (kJ mol^{-1})	$\bar{H}_{w,COSMO}^{E,\infty}$ (kJ mol^{-1})	ARD (%)
[C_4mim][CF_3SO_3]	3.8 ± 0.2	3.7 ± 0.1	0.3
[C_4mim][SCN]	−0.8 ± 0.1	−0.6 ± 0.2	29.4
[C_4mim][TFA]	−3.9 ± 0.1	−5.1 ± 0.4	29.7
[C_4mim]Br	−11.1 ± 0.9	−3.3 ± 0.1	70.6
[C_4mim][TOS]	−2.8 ± 0.2	−4.1 ± 0.1	50.7
[C_4mim]Cl	−9.0 ± 0.2	−10.7 ± 0.2	18.9
[C_4mim][CH_3SO_3]	−4.9 ± 0.4	−6.7 ± 0.3	37.0
[C_4mim][DMP]	−11.0 ± 0.3	−11.4 ± 0.5	4.1
[C_4mim][Ac]	−12.0 ± 0.4	−20.0 ± 0.7	67.2
average			34.2

3.3. COSMO-RS Description for Pure Compound. An advantage of COSMO-RS when compared to other thermodynamic g^E models is that it provides information regarding the molecular interactions that can be visualized in the so-called σ-profile and σ-potential. As an example, Figure 7 presents the σ-profile and σ-potential of water, [C_4mim]Cl, and [C_4mim]Br. The two vertical dotted lines are the locations of the cutoff values for the hydrogen bond donor (σ_{HB} < −1.0 e nm^{-2}) and acceptor (σ_{HB} > 1.0 e nm^{-2}). The importance of this cutoff value indicates that any molecule with σ-profile lying at the left side of −1.0 e nm^{-2} will have H-bond donor ability while those at the right side of 1.0 e nm^{-2} will have acceptor ability. Profiles lying at the negative region are due to inherent positive charge of the atom or molecule and vice versa for the positive region of profile. The σ-profile of water (Figure 7a) is very broad, covering negative, positive, and neutral area (from −2.0 to 2.1 e nm^{-2}). On the negative side, the peak at −1.6 e nm^{-2} is assigned to the two polar hydrogen atoms, whereas the broad peak on the positive side at 1.8 e nm^{-2} results from the two pairs of electrons of the oxygen atom. Apart from small fluctuations, the σ-profile of water is almost symmetric and is of high importance for the properties of water because the symmetry

dx.doi.org/10.1021/jp4113552 | J. Phys. Chem. B 2014, 118, 1848−1860

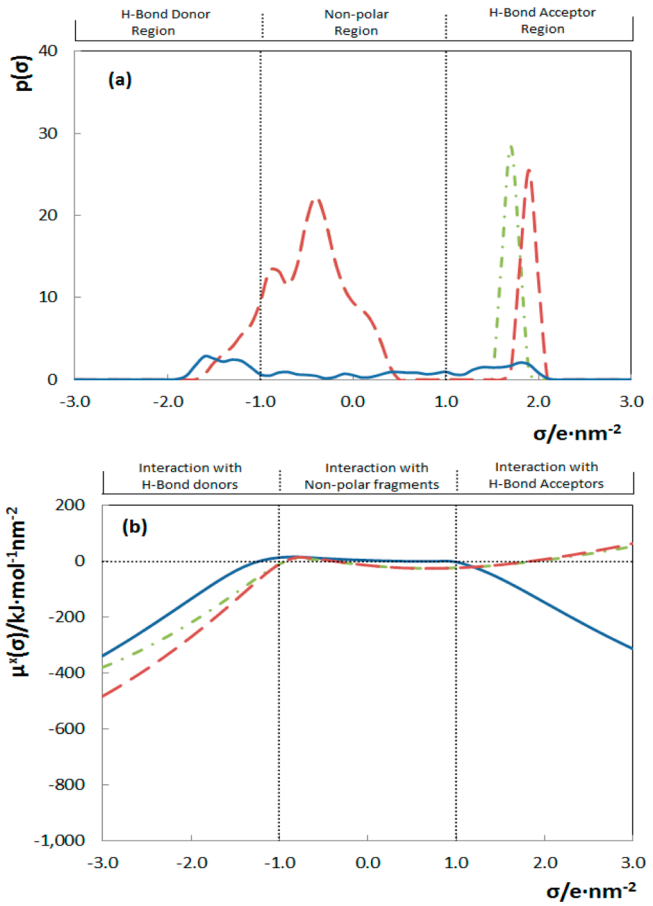

Figure 7. σ-Profile (a) and σ-potential (b) of water (solid line), $[C_4mim]Cl$ (dashed line), and $[C_4mim]Br$ (dashed and dotted line).

implies a balance between the positive and negative charges on the surface of this compound. Regarding the σ-potential of water, the symmetry is even more evident, indicating that water can act equally as both H-bond donor and acceptor. Because the oxygen atom of one water molecule has two lone pairs of electron, each of which can form a hydrogen bond with a hydrogen atom of another water molecule, they can create a strong three-dimensional hydrogen bond network.[53,54] This hydrogen-bond network is the dominant energy that governs the stability of water (H_{HB} of water is -27.70 kJ·mol^{-1}, Table 3).

Unlike water, the sigma profile of ionic liquids is highly asymmetric (Figures 7 and 8 and Figures S1 and S2 in Supporting Information). The $[C_4mim]^+$ cation occupies the negative and almost entire nonpolar area, while the anion is positioned far away in the positive area. The cation presents a shoulder-like peak at -0.9 e nm^{-2}, attributed to the acidic hydrogen atom in the imidazolium ring that could act as a very weak H-bond donor. The capability of this acidic hydrogen to form hydrogen bonding with the ionic liquid anions counterpart has been proven experimentally using ^{1}H NMR,[8,9,55] infrared spectra,[56] Raman and ab initio calculation.[57] Thus, the acidic hydrogen in the imidazolium ring plays an important role as H-bond donor with the anion counterpart.

Regarding the σ-profile of the anion, a peak with high intensity at 1.9 e nm^{-2} is related to the four pairs of electrons of Cl^-. Each electron pair in Cl^- can form a hydrogen bond with a H-bond donor. Because the $[C_4mim]^+$ cation can provide only one (acidic) hydrogen atom (of the imidazolium ring), additional donors are highly desired, as can be seen from the σ-potential of $[C_4mim]Cl$. In the σ-potential, the asymmetry is even more obvious, indicating uneven charge distribution within ionic liquid molecules. On the negative side, $[C_4mim]Cl$ shows attraction to H-bond donor resulting from the lone pairs of electrons in the Cl^- anion. But on the positive side, because of the lack of an H-bond donor among ionic liquid molecules, they present repulsion toward another H-bond acceptor functionality because this would compete with the existing acceptor for the rare H-bond donor. COSMO-RS translates this into the electrostatic-misfit interaction energy, H_{MF}, which is highly important to the total energy of ionic liquids (Table 3). All the studied ionic liquids present high and positive H_{MF} due to a lack of H-bond donors, displaying high attraction toward H-bond donors. Consequently, another solute or solvent with H-bond donors (like water) will favorably interact with these ionic liquids. A closer look at Table 3 reveals that the dominant interactions that exist in the pure ionic liquid are the van der Walls forces. The hydrogen bond contribution is also found to be negative, indicating the existence of hydrogen bonding between ionic liquid cation and anion. The endothermic contribution of electrostatic-misfit interaction, as previously discussed, arises from the unbalanced number of hydrogen bond donors and acceptors among ionic liquid molecules.

Figure 7 also shows the behavior of $[C_4mim]Br$. The σ-profile of $[C_4mim]Br$ within the negative and nonpolar region is similar to that of $[C_4mim]Cl$. On the positive area, the peak for Br^- (at 1.7 e nm^{-2}) is in the left side of Cl^-. This is due to the fact that both Cl^- and Br^- have four pairs of lone electrons, but the latter has a larger size, presenting a lower negative charge density surrounding the anion. This explains the fact that $[C_4mim]^+$ presents a hydrogen bond with Br^- that is weaker than that with Cl^- and a lower electrostatic-misfit interaction energy (Table 3). Consequently, it is also expected that $[C_4mim]Br$ will have an interaction with water that is lower than that of $[C_4mim]Cl$.

The σ-profile of $[C_4mim][Ac]$ has a wider area in the positive region (Figure 8), up to a maximum 3.0 e nm^{-2}. A broader peak at 2.1 e nm^{-2} assigned to $[Ac]^-$ and located on the right side of Cl^- indicates that the former anion has a higher negative charge density due to the presence of five pairs of lone electrons. Consequently, the $[C_4mim]^+$ has stronger hydrogen bonding with $[Ac]^-$ than with Cl^-, as displayed in their hydrogen bond energy, H_{HB}. Like Cl^-, the $[Ac]^-$ in $[C_4mim][Ac]$ is also "unsaturated", with five sites available for accepting H-bonds, but only one H-bond donor comes from the cation. Therefore, $[C_4mim][Ac]$ also displays an attraction toward an H-bond donor. Figure 8 also shows the effect of fluorination of the $[Ac]^-$ in the case of $[TFA]^-$. The fluorination caused the peak within the positive area to shift left, indicating that the charge density of $[TFA]^-$ is less negative than that of the $[Ac]^-$ anion. Consequently, the $[C_4mim]^+$ has a lesser hydrogen bonding interaction with the $[TFA]^-$. Despite the fluorination reducing the negative charge density of $[C_4mim][TFA]$, this ionic liquid also presents high attraction to a H-bond donor, for the same reason as the $[C_4mim][Ac]$. The effect of fluorination of $[CH_3SO_3]^-$ into $[CF_3SO_3]^-$ also reduces the negative charge density of the fluorinated anion, as displayed by their corresponding peaks in the positive area, at 1.8 and 1.4, respectively (Figure S1 of Supporting Information). In addition, Figure S1 also shows the effect of substituting the H_3C- group of $[CH_3SO_3]^-$ with an aromatic ring to form $[TOS]^-$. The substitution shifts the peak to the positive area slightly to left and causes the appearance of extra peaks in the

dx.doi.org/10.1021/jp4113552 | J. Phys. Chem. B 2014, 118, 1848−1860

Table 3. Enthalpies of Interaction of Water and Ionic Liquids at 298.2 K Estimated by COSMO-RS

molecule	H_i (kJ mol^{-1})	$H_{i,MF}$ (kJ mol^{-1})	$H_{i,HB}$ (kJ mol^{-1})	$H_{i,vdW}$ (kJ mol^{-1})
H_2O	−29.48	1.36	−27.70	−3.14
$[C_4mim][CF_3SO_3]$	−37.51	33.82	−16.71	−55.65
$[C_4mim]^+$	−21.83	22.33	−8.37	−35.79
$[CF_3SO_3]^-$	−16.72	11.49	−8.34	−19.86
$[C_4mim][SCN]$	−39.90	36.10	−16.64	−59.36
$[C_4mim]^+$	−21.21	27.38	−8.34	−41.25
$[SCN]^-$	−17.69	8.71	−8.30	−18.11
$[C_4mim][TFA]$	−39.35	37.24	−23.93	−52.67
$[C_4mim]^+$	−22.32	25.64	−12.00	−35.96
$[TFA]^-$	−17.03	11.60	−11.93	−16.70
$[C_4mim]Br$	−30.39	51.25	−25.22	−56.43
$[C_4mim]^+$	−17.31	37.99	−12.64	−42.66
Br^-	−13.08	13.27	−12.58	−13.77
$[C_4mim][TOS]$	−48.48	49.75	−24.59	−73.64
$[C_4mim]^+$	−23.43	26.60	−12.31	−38.71
$[TOS]^-$	−24.05	23.15	−12.28	−34.93
$[C_4mim]Cl$	−26.44	57.39	−30.34	−53.49
$[C_4mim]^+$	−15.30	41.68	−15.21	−41.77
Cl^-	−11.14	15.71	−15.14	−11.72
$[C_4mim][CH_3SO_3]$	−35.40	51.10	−28.58	−57.91
$[C_4mim]^+$	−20.07	32.78	−14.24	−38.60
$[CH_3SO_3]^-$	−15.33	18.32	−14.34	−19.31
$[C_4mim][DMP]$	−43.87	53.52	−32.35	−65.03
$[C_4mim]^+$	−23.55	31.47	−16.21	−38.82
$[DMP]^-$	−20.31	22.04	−16.14	−26.21
$[C_4mim][Ac]$	−39.94	55.32	−39.72	−55.53
$[C_4mim]^+$	−21.97	36.97	−19.92	−39.03
$[Ac]^-$	−17.96	18.35	−19.80	−16.51

nonpolar region. Hence, the hydrogen bonding between $[C_4mim]$ and $[TOS]$ is weaker than that of $[C_4mim][CH_3SO_3]$. It is also interesting to compare the effect of fluorination and aromatization of the anion; it seems that the former has more impact on the charge density of the sulfonate-core head. This might be related to the strong electron-drawing ability of the fluorine atom.[58]

This discussion of σ-profiles and σ-potentials suggests that the COSMO-RS supplies a vivid and rich depiction of the ionic liquids and water as well as their behavior in a pure state, allowing us to anticipate the likely interactions that will occur in the presence of other solutes or solvents. As can be observed from Figures 7 and 8, Figures S1 and S2 in Supporting Information, and Table 3 that because the cation can donate only one H-bond, whereas the anion counterpart can accept more than one H-bond, highly electrostatic misfit of the ionic liquids is observed. This leads to high attraction of the ionic liquid toward the H-bond donor, such as water. The following section discusses the interaction of water with the ionic liquids based on the estimated excess enthalpy using COSMO-RS.

3.4. Binary Mixtures of H_2O and Ionic Liquids. In a previous work we established the reliability of COSMO-RS to predict the excess enthalpies of binary mixtures composed of ionic liquids and water.[25] Unfortunately, there are no experimental excess enthalpy data for the systems studied here, but the capability of the model to describe the activity coefficient data shown in the previous sections, the highly consistent conclusions found in our previous work following a similar approach, and the capability to describe the excess enthalpies[22,25] give us confidence in using COSMO-RS to further characterize the interactions between the water and the ionic liquids. Figure 9 presents the estimated excess enthalpies of binary mixtures of ionic liquids and water. As previously mentioned, the unbalanced number of H-bond donors and acceptors of the ionic liquids is the reason for high attraction of these compounds toward H-bond donors, such as water. As a consequence, the presence of water reduces the electrostatic misfit between cation and anion and at the same time establishment of new hydrogen bonding between cation−water and anion−water. As can be seen from Table S2 in Supporting Information, the hydrogen bonding contribution of anion−water is the key factor in the interaction of most ionic liquids and water. Generally, the new established hydrogen bonding between anion−water could cover the hydrogen bond lost between water molecule, which translates to negative excess enthalpy. On the contrary, the small positive excess enthalpy of $[C_4mim][CF_3SO_3]$ (for water-rich compositions) indicates that the hydrogen bond between $[CF_3SO_3]^-$−water is energetically weak and could not impose the hydrogen bond lost by water during mixing. To regain the lost hydrogen bonding network, the water molecules tend to use the energy of the system to reorient themselves.[59,60] This suggests that the solubility of water, within $x_{H_2O} \leq 0.5$, in $[C_4mim][CF_3SO_3]$ is an endothermic process and entropically driven. Such phenomena have also been observed for the solubility of $[Tf_2N]$-based ionic liquids[52] and are in agreement with the observed dependency of the infinite dilution activity coefficients with temperature already discussed.

A closer look into Figure 9a (and Table S2 of Supporting Information) could reveal the mechanism taking place during dissolution of water in the ionic liquids. For example, in the system of binary mixtures of (H_2O + $[C_4mim]Cl$), as discussed in the σ-potential, pure ionic liquids have high attraction to the

dx.doi.org/10.1021/jp4113552 | J. Phys. Chem. B 2014, 118, 1848−1860

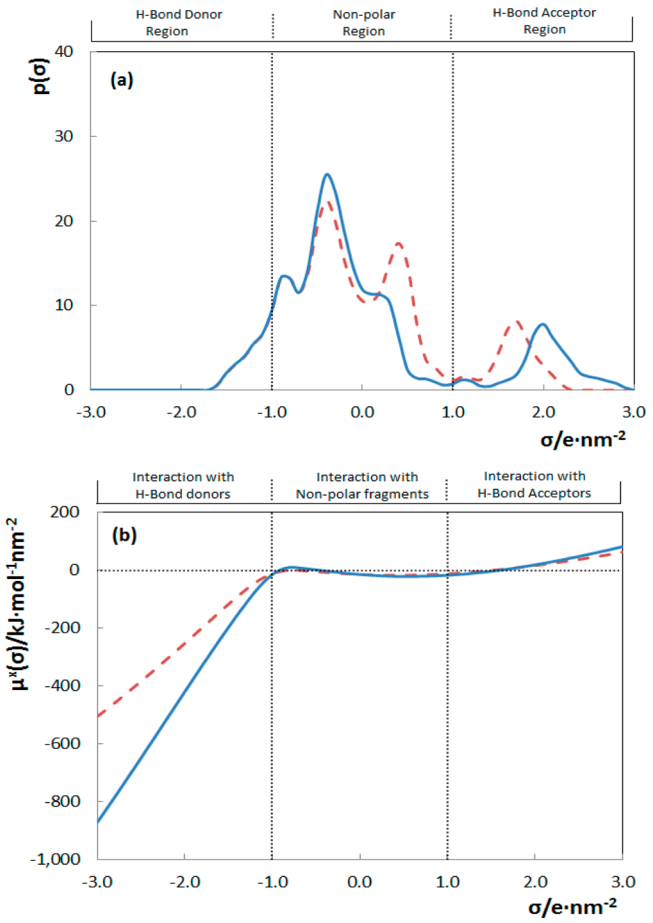

Figure 8. σ-Profile (a) and σ-potential (b) of [C_4mim][Ac] (solid line) and [C_4mim][TFA] (dashed line).

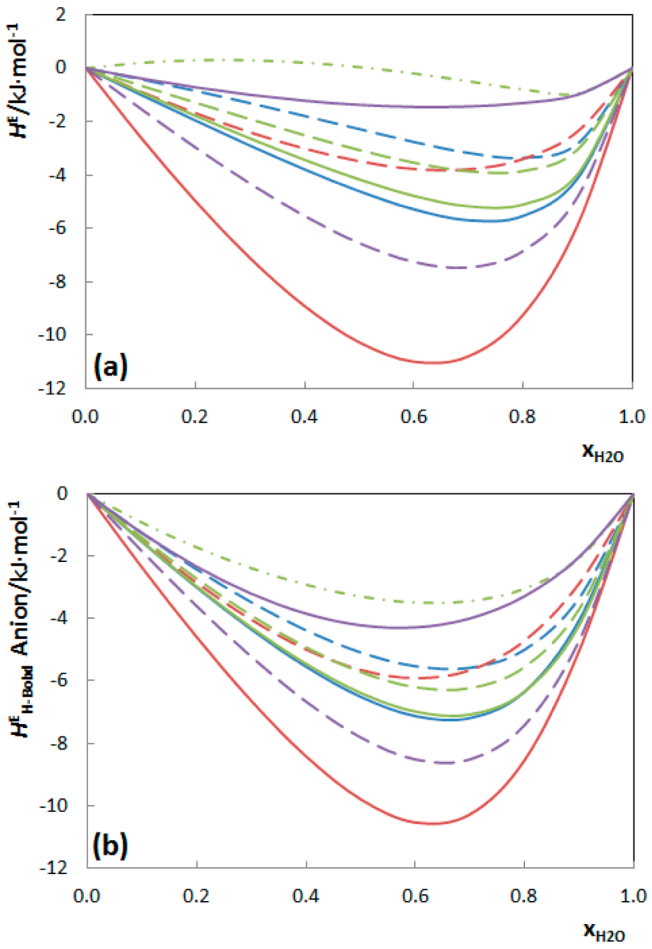

Figure 9. Total (a) and contribution of hydrogen bonding of anion (b) to the excess enthalpies of binary mixtures of ionic liquids and water at 298.2 K estimated by COSMO-RS. Solid blue line, [C_4mim]Cl; dashed blue line, [C_4mim]Br; solid red line, [C_4mim]-[Ac]; dashed red line, [C_4mim][TFA]; solid green line, [C_4mim]-[CH_3SO_3]; dashed green line, [C_4mim][TOS]; dashed and dotted green line, [C_4mim][CF_3SO_3]; solid purple line, [C_4mim][SCN]; dashed purple line, [C_4mim][DMP].

H-bond donor group. The polar hydrogen of water surges very well to the lone pairs of electrons of the Cl^- anion. The addition of H_2O reduces the electrostatic interaction between the $[C_4mim]^+$ cation and Cl^- anion; both of these ions are attracted to H_2O, as displayed from the negative contribution of H^E_{MF} of the cation and anion. At low concentration, some of the water molecule is hydrogen bonded, most probably to the ionic liquid anion counterpart. As the water content increases, more and more water molecules gather around anions until it reaches a limit at which the hydrogen bonding of the Cl^-anions is "saturated". Subsequently, the addition of more water causes the turnover point; the water−water interactions dominate, causing the water−water interaction to be closer to that of the neat system. In Figure 9a, it can be seen that the turnover point is reached at $x_{H_2O} \sim 0.75$, equal to one molecule of ionic liquid and three molecules of water. Despite the fact that the Cl^- anion has four pairs of lone electrons, one is already taken by $[C_4mim]^+$ cation, and it seems that Cl^- anions form "a complex" with three molecules of water while maintaining the hydrogen bonding with the $[C_4mim]^+$ cation. It should be highlighted that this finding has been reported by Niazi and co-worker[17] making use of molecular dynamics solution of [C_4mim]Cl−H_2O systems. They showed that there is an average of three molecules of water per one Cl^- anion at 0.75 molar fraction of water.[17] Thus, there is good agreement between the molecular dynamics and COSMO-RS approaches.

It should be noted that that the number of water molecules forming a complex with the anion is strongly dependent on the nature of the anion itself, but as is shown by refs 2,7,17, and 18, these findings confirm that the hydrogen bonding of anion and water governs the water and ionic liquid interaction.

Analyzing the contribution of each specific interaction to the total excess enthalpy of ionic liquid and water, as depicted in Figure 10, reveals that at $x_{H_2O} = 0.66$, the dominant interaction, as expected, is the hydrogen bonding that contributes 41.7−85.5% of the total excess enthalpy. Even with the system of H_2O + [C_4mim][CF_3SO_3], hydrogen bonding is still the dominant interaction. The trend of hydrogen bonding contribution to the total excess enthalpy, as previously discussed, is in close agreement with the hydrogen bonding basicity taken from the solvatochromic parameter.[61,62] On the contrary, no trend of electrostatic misfit and van der Walls contribution is observed. The results suggest, in agreement with previous reports using other techniques,[7−13,15−20] that the dominant interaction in these systems is the hydrogen bonding of water and the ionic liquid anion (Table S2 of Supporting Information). Accordingly, the anion can be ranked as $[CF_3SO_3]^-$ < $[SCN]^-$ < $[TFA]^-$ < Br^- < $[TOS]^-$ < Cl^- < $[CH_3SO_3]^-$ < $[DMP]^-$ < $[Ac]^-$. This pattern closely follows the trend observed in the activity

dx.doi.org/10.1021/jp4113552 | J. Phys. Chem. B 2014, 118, 1848−1860

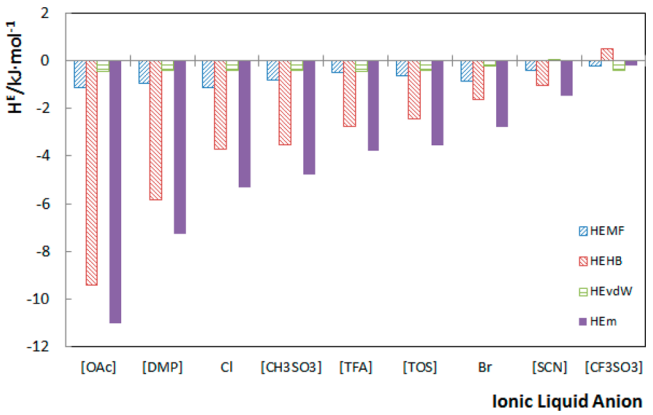

Figure 10. Contribution of specific interaction to the total excess enthalpy.

coefficient of water in the ionic liquids and the hydrogen bond basicity of [C_4mim]-based ionic liquids regarding their anion. The hydrogen bond basicity expressed by the β solvatochromic parameter, according to the ionic liquid anion nature, follows the sequence $[CF_3SO_3]^-$ < $[SCN]^-$ < $[TFA]^-$ < Br^- < $[TOS]^-$ < Cl^-< $[CH_3SO_3]^-$ < $[DMP]^-$ < $[Ac]^-$.[61,62] Therefore, it can be concluded that the interaction of water and ionic liquids is controlled by the hydrogen bond basicity of the respective anion.

4. CONCLUSION

The knowledge of ionic liquid interaction with other solute or solvents is a key requirement for designing ionic liquids for specific purposes. We have performed extensive experimental and quantum chemical modeling for [C_4mim]-based ionic liquids, the most frequently studied in the literature, with nine different anions. Despite the failure of COSMO-RS to describe the correct trend of the activity coefficient of water in the ionic liquids [C_4mim][CF_3SO_3] and [C_4mim][SCN], it is still able to correctly rank the anion as observed experimentally and also able to forecast the impact of fluorination and aromatization of the anion. The estimated excess enthalpy analysis of the binary system reveals that the interaction of ionic liquids and water was governed by the basicity of the anion. Furthermore, deeper analysis of the binary mixture of H_2O and [C_4mim]Cl reveals the formation of a complex between the anion and three molecules of water.

The effect of temperature on the activity coefficient of water at infinite dilution in the ionic liquids was also studied. In general, the activity coefficient of water at infinite dilution increases with increasing temperature. This is due to less exothermic process occurring at higher temperature. The only exception was observed for the activity coefficient of water at infinite dilution in [C_4mim][CF_3SO_3], in which the value decreased with increasing temperature, showing the dissolution of water in this ionic liquid is endothermic and entropically driven. The results obtained indicate that the proper selection of anion of the ionic liquids presents a very interesting opportunity for expanding the capabilities of these solvents and the number of applications where binary mixture of ionic liquids and water might find use in the future.

■ ASSOCIATED CONTENT

Supporting Information

Equation for calculating the average relative deviation (ARD) (eq S1); σ-profile and potential of [C_4mim][CH_3SO_3], [C_4mim][CF_3SO_3], and [C_4mim][TOS] (Figure S1); σ-profile and potential of [C_4mim][SCN] and [C4mim][DMP] (Figure S2); experimental and predicted activity coefficient of water at infinite dilution in ionic liquids using COSMO-RS along with the deviation calculated using eq S1 (Table S1); and contribution of specific interaction of each molecule to the excess enthalpy of binary mixture of H_2O and ionic liquids at 298.2 K estimated by COSMO-RS (Table S2). This material is available free of charge via the Internet at http://pubs.acs.org.

■ AUTHOR INFORMATION

Corresponding Author

*Tel.: +351 234 401 507. Fax: + 351 234 370 084. E-mail: jcoutinho@ua.pt.

Notes

The authors declare no competing financial interest.

■ ACKNOWLEDGMENTS

This work was financed by national funding from Fundação para a Ciência e a Tecnologia (FCT, Portugal), European Union, QREN, FEDER, and COMPETE for funding the CICECO (project PEst-C/CTM/LA0011/2013), QOPNA (project PEst-C/QUI/UI0062/2013), and LSRE/LCM (project PEst-C/EQB/LA0020/2013). I.K. and K.A.K. acknowledge FCT for the postdoctoral grants SFRH/BPD/76850/2011 and SFRH/BPD/88101/2012, respectively.

■ REFERENCES

(1) Freire, M. G.; Neves, C. M. S. S.; Carvalho, P. J.; Gardas, R. L.; Fernandes, A. M.; Marrucho, I. M.; Santos, L. M. N. B. F.; Coutinho, J. A. P. Mutual Solubilities of Water and Hydrophobic Ionic Liquids. *J. Phys. Chem. B* **2007**, *111* (45), 13082−13089.

(2) Xu, M.; Ivey, D. G.; Xie, Z.; Qu, W.; Dy, E. The state of water in 1-butly-1-methyl-pyrrolidinium bis(trifluoromethanesulfonyl)imide and its effect on Zn/Zn(II) redox behavior. *Electrochim. Acta* **2013**, *97*, 289−295.

(3) Dong, L.; Zheng, D.; Li, J.; Nie, N.; Wu, X. Suitability prediction and affinity regularity assessment of H_2O + imidazolium ionic liquid working pairs of absorption cycle by excess property criteria and UNIFAC model. *Fluid Phase Equilib.* **2013**, *348* (0), 1−8.

(4) Zheng, D.; Dong, L.; Wu, X. New Approach for Absorbent Species Selection with Excess Gibbs Function. *Ind. Eng. Chem. Res.* **2013**, *52* (27), 9480−9489.

(5) Khamooshi, M.; Parham, K.; Atikol, U. Overview of ionic liquids used as working fluids in absorption cycles. *Adv. Mech. Eng.* **2013**, *2013*, 1−7.

(6) Shiflett, M. B.; Niehaus, A. M. S.; Elliott, B. A.; Yokozeki, A. Phase Behavior of N_2O and CO_2 in Room-Temperature Ionic Liquids [bmim][Tf_2N], [bmim][BF_4], [bmim][$N(CN)_2$], [bmim][Ac], [eam][NO_3], and [bmim][SCN]. *Int. J. Thermophys.* **2012**, *33* (3), 412−436.

(7) Cammarata, L.; Kazarian, S. G.; Salter, P. A.; Welton, T. Molecular states of water in room temperature ionic liquids. *Phys. Chem. Chem. Phys.* **2001**, *3* (23), 5192−5200.

(8) Huang, J.-F.; Chen, P.-Y.; Sun, I. W.; Wang, S. P. NMR evidence of hydrogen bonding in 1-ethyl-3-methylimidazolium-tetrafluoroborate room temperature ionic liquid. *Inorg. Chim. Acta* **2001**, *320* (1−2), 7−11.

(9) Mele, A.; Tran, C. D.; De Paoli Lacerda, S. H. The Structure of a Room-Temperature Ionic Liquid with and without Trace Amounts of Water: The Role of C[BOND]H···O and C[BOND]H···F Interactions in 1-*n*-Butyl-3-Methylimidazolium Tetrafluoroborate. *Angew. Chem., Int. Ed.* **2003**, *42* (36), 4364−4366.

(10) Dwan, J.; Durant, D.; Ghandi, K. Nuclear magnetic resonance spectroscopic studies of the trihexyl (tetradecyl) phosphonium

chloride ionic liquid mixtures with water. *Cent. Eur. J. Chem.* **2008**, *6* (3), 347−358.
(11) Zhang, Q.-G.; Wang, N.-N.; Yu, Z.-W. The Hydrogen Bonding Interactions between the Ionic Liquid 1-Ethyl-3-Methylimidazolium Ethyl Sulfate and Water. *J. Phys. Chem. B* **2010**, *114* (14), 4747−4754.
(12) Fumino, K.; Wulf, A.; Ludwig, R. The potential role of hydrogen bonding in aprotic and protic ionic liquids. *Phys. Chem. Chem. Phys.* **2009**, *11* (39), 8790−8794.
(13) Hanke, C. G.; Lynden-Bell, R. M. A Simulation Study of Water-Dialkylimidazolium Ionic Liquid Mixtures. *J. Phys. Chem. B* **2003**, *107* (39), 10873−10878.
(14) Katayanagi, H.; Nishikawa, K.; Shimozaki, H.; Miki, K.; Westh, P.; Koga, Y. Mixing Schemes in Ionic Liquid−H_2O Systems: A Thermodynamic Study. *J. Phys. Chem. B* **2004**, *108* (50), 19451−19457.
(15) Jiang, W.; Wang, Y.; Voth, G. A. Molecular Dynamics Simulation of Nanostructural Organization in Ionic Liquid/Water Mixtures. *J. Phys. Chem. B* **2007**, *111* (18), 4812−4818.
(16) Wang, N.-N.; Zhang, Q.-G.; Wu, F.-G.; Li, Q.-Z.; Yu, Z.-W. Hydrogen Bonding Interactions between a Representative Pyridinium-Based Ionic Liquid [BuPy][BF_4] and Water/Dimethyl Sulfoxide. *J. Phys. Chem. B* **2010**, *114* (26), 8689−8700.
(17) Niazi, A. A.; Rabideau, B. D.; Ismail, A. E. Effects of Water Concentration on the Structural and Diffusion Properties of Imidazolium-Based Ionic Liquid−Water Mixtures. *J. Phys. Chem. B* **2013**, *117* (5), 1378−1388.
(18) Aparicio, S.; Alcalde, R.; Atilhan, M. Experimental and Computational Study on the Properties of Pure and Water Mixed 1-Ethyl-3-methylimidazolium L-(+)-Lactate Ionic Liquid. *J. Phys. Chem. B* **2010**, *114* (17), 5795−5809.
(19) Crowhurst, L.; Mawdsley, P. R.; Perez-Arlandis, J. M.; Salter, P. A.; Welton, T. Solvent-solute interactions in ionic liquids. *Phys. Chem. Chem. Phys.* **2003**, *5* (13), 2790−2794.
(20) Weingärtner, H. Understanding ionic liquids at the molecular level: Facts, problems, and controversies. *Angew. Chem., Int. Ed.* **2008**, *47* (4), 654−670.
(21) Anantharaj, R.; Banerjee, T. Quantum chemical studies on the simultaneous interaction of thiophene and pyridine with ionic liquid. *AIChE J.* **2010**, *57* (3), 749−764.
(22) Navas, A.; Ortega, J.; Vreekamp, R.; Marrero, E.; Palomar, J. Experimental Thermodynamic Properties of 1-Butyl-2-methylpyridinium Tetrafluoroborate [b2mpy][BF_4] with Water and with Alkan-1-ol and Their Interpretation with the COSMO-RS Methodology. *Ind. Eng. Chem. Res.* **2009**, *48* (5), 2678−2690.
(23) Gonzalez-Miquel, M.; Palomar, J.; Rodriguez, F. Selection of Ionic Liquids for Enhancing the Gas Solubility of Volatile Organic Compounds. *J. Phys. Chem. B* **2013**, *117* (1), 296−306.
(24) Zhou, T.; Chen, L.; Ye, Y.; Qi, Z.; Freund, H.; Sundmacher, K. An overview of mutual solubility of ionic liquids and water predicted by COSMO-RS. *Ind. Eng. Chem. Res.* **2012**, *51* (17), 6256−6264.
(25) Kurnia, K. A.; Coutinho, J. A. P. Overview of the Excess Enthalpies of the Binary Mixtures Composed of Molecular Solvents and Ionic Liquids and Their Modeling using COSMO-RS. *Ind. Eng. Chem. Res.* **2013**, *52* (38), 13862−13874.
(26) Anantharaj, R.; Banerjee, T. COSMO-RS-Based Screening of Ionic Liquids as Green Solvents in Denitrification Studies. *Ind. Eng. Chem. Res.* **2010**, *49* (18), 8705−8725.
(27) Anantharaj, R.; Banerjee, T. COSMO-RS based predictions for the desulphurization of diesel oil using ionic liquids: Effect of cation and anion combination. *Fuel Process. Technol.* **2011**, *92* (1), 39−52.
(28) Palomar, J.; Gonzalez-Miquel, M.; Polo, A.; Rodriguez, F. Understanding the Physical Absorption of CO_2 in Ionic Liquids Using the COSMO-RS Method. *Ind. Eng. Chem. Res.* **2011**, *50* (6), 3452−3463.
(29) Casas, A.; Omar, S.; Palomar, J.; Oliet, M.; Alonso, M. V.; Rodriguez, F. Relation between differential solubility of cellulose and lignin in ionic liquids and activity coefficients. *RSC Adv.* **2013**, *3* (10), 3453−3460.
(30) Freire, M. G.; Ventura, S. P. M.; Santos, L. M. N. B. F.; Marrucho, I. M.; Coutinho, J. A. P. Evaluation of COSMO-RS for the prediction of LLE and VLE of water and ionic liquids binary systems. *Fluid Phase Equilib.* **2008**, *268* (1−2), 74−84.
(31) Freire, M. G.; Santos, L. M. N. B. F.; Marrucho, I. M.; Coutinho, J. A. P. Evaluation of COSMO-RS for the prediction of LLE and VLE of alcohols + ionic liquids. *Fluid Phase Equilib.* **2007**, *255* (2), 167−178.
(32) Ferreira, A. R.; Freire, M. G.; Ribeiro, J. C.; Lopes, F. M.; Crespo, J. G.; Coutinho, J. A. P. An Overview of the Liquid−Liquid Equilibria of (Ionic Liquid + Hydrocarbon) Binary Systems and Their Modeling by the Conductor-like Screening Model for Real Solvents. *Ind. Eng. Chem. Res.* **2011**, *50* (9), 5279−5294.
(33) Ferreira, A. R.; Freire, M. G.; Ribeiro, J. C.; Lopes, F. M.; Crespo, J. G.; Coutinho, J. A. P. Overview of the liquid−liquid equilibria of ternary systems composed of ionic liquid and aromatic and aliphatic hydrocarbons, and their modeling by COSMO-RS. *Ind. Eng. Chem. Res.* **2012**, *51* (8), 3483−3507.
(34) Freire, M. G.; Neves, C. M. S. S.; Carvalho, P. J.; Gardas, R. L.; Fernandes, A. M.; Marrucho, I. M.; Santos, L. M. N. B. F.; Coutinho, J. A. P. Mutual Solubilities of Water and Hydrophobic Ionic Liquids. *J. Phys. Chem. B* **2007**, *111* (45), 13082−13089.
(35) Freire, M. G.; Carvalho, P. J.; Gardas, R. L.; Marrucho, I. M.; Santos, L. M. N. B. F.; Coutinho, J. A. P. Mutual Solubilities of Water and the [$C_n$mim][Tf_2N] Hydrophobic Ionic Liquids. *J. Phys. Chem. B* **2008**, *112* (6), 1604−1610.
(36) Khan, I.; Kurnia, K. A.; Sintra, T. E.; Saraiva, J. A.; Pinho, S. P.; Coutinho, J. A. P. Assessing the activity coefficients of water in cholinium-based ionic liquids: Experimental measurements and COSMO-RS modeling. *Fluid Phase Equilib.* **2014**, *361*, 16−22.
(37) Passos, H.; Khan, I.; Mutelet, F.; Oliveira, M. B.; Carvalho, P. J.; Santos, L. M. N. B. F.; Held, C.; Sadowski, G.; Freire, M. G.; Coutinho, J. A. P. Vapor−Liquid Equilibria of Water + Alkylimidazolium-based Ionic Liquids: Measurements and PC-SAFT Modeling. *Ind. Eng. Chem. Res.*
(38) Archer, D. G. Thermodynamic properties of the KCl + H_2O system. *J. Phys. Chem. Ref. Data* **1999**, *28* (1), 1−17.
(39) Rard, J. A.; Clegg, S. L. Critical Evaluation of the Thermodynamic Properties of Aqueous Calcium Chloride. 1. Osmotic and Activity Coefficients of 0−10.77 mol·kg^{-1} Aqueous Calcium Chloride Solutions at 298.15 K and Correlation with Extended Pitzer Ion-Interaction Models. *J. Chem. Eng. Data* **1997**, *42* (5), 819−849.
(40) Cruickshank, A. J. B.; Windsor, M. L.; Young, C. L. The Use of Gas-liquid Chromatography to Determine Activity Coefficients and Second Virial Coefficients of Mixtures. I. Theory and Verification of Method of Data Analysis. *Proc. R. Soc. A* **1966**, *295* (1442), 259−270.
(41) Cruickshank, A. J. B.; Windsor, M. L.; Young, C. L. The Use of Gas-liquid Chromatography to Determine Activity Coefficients and Second Virial Coefficients of Mixtures. II. Experimental Studies on Hydrocarbon Solutes. *Proc. R. Soc. A* **1966**, *295* (1442), 271−287.
(42) Revelli, A.-L.; Sprunger, L. M.; Gibbs, J.; Acree, W. E.; Baker, G. A.; Mutelet, F. Activity Coefficients at Infinite Dilution of Organic Compounds in Trihexyl(tetradecyl)phosphonium Bis-(trifluoromethylsulfonyl)imide using Inverse Gas Chromatography. *J. Chem. Eng. Data* **2009**, *54* (3), 977−985.
(43) Klamt, A. *COSMO-RS from Quantum Chemistry to Fluid Phase Thermodynamics and Drug Design*. Elsevier: Amsterdam, The Netherlands, 2005.
(44) Eckert, F.; Klampt, A. COSMOtherm, version C2.1, release 01.08; COSMOlogic GmbH & Co. KG: Leverkusen, Germany, 2006.
(45) Diedenhofen, M.; Eckert, F.; Klamt, A. Prediction of Infinite Dilution Activity Coefficients of Organic Compounds in Ionic Liquids Using COSMO-RS. *J. Chem. Eng. Data* **2003**, *48* (3), 475−479.
(46) Putnam, R.; Taylor, R.; Klamt, A.; Eckert, F.; Schiller, M. Prediction of Infinite Dilution Activity Coefficients Using COSMO-RS. *Ind. Eng. Chem. Res.* **2003**, *42* (15), 3635−3641.
(47) Domanska, U.; Laskowska, M. Measurements of activity coefficients at infinite dilution of aliphatic and aromatic hydrocarbons, alcohols, thiophene, tetrahydrofuran, MTBE, and water in ionic liquid

[BMIM][SCN] using GLC. *J. Chem. Thermodyn.* **2009**, *41* (5), 645−650.
(48) Domańska, U.; Marciniak, A. Activity Coefficients at Infinite Dilution Measurements for Organic Solutes and Water in the Ionic Liquid 1-Butyl-3-methylimidazolium Trifluoromethanesulfonate. *J. Phys. Chem. B* **2008**, *112* (35), 11100−11105.
(49) Domańska, U.; Redhi, G. G.; Marciniak, A. Activity coefficients at infinite dilution measurements for organic solutes and water in the ionic liquid 1-butyl-1-methylpyrrolidinium trifluoromethanesulfonate using GLC. *Fluid Phase Equilib.* **2009**, *278* (1−2), 97−102.
(50) Marciniak, A.; Wlazlo, M. Activity Coefficients at Infinite Dilution Measurements for Organic Solutes and Water in the Ionic Liquid 1-Butyl-3-methyl-pyridinium Trifluoromethanesulfonate. *J. Chem. Eng. Data* **2010**, *55* (9), 3208−3211.
(51) Miki, K.; Westh, P.; Nishikawa, K.; Koga, Y. Effect of an "Ionic Liquid" Cation, 1-Butyl-3-methylimidazolium, on the Molecular Organization of H_2O. *J. Phys. Chem. B* **2005**, *109* (18), 9014−9019.
(52) Freire, M. G.; Neves, C. M. S. S.; Ventura, S. P. M.; Pratas, M. J.; Marrucho, I. M.; Oliveira, J.; Coutinho, J. A. P.; Fernandes, A. M. Solubility of non-aromatic ionic liquids in water and correlation using a QSPR approach. *Fluid Phase Equilib.* **2010**, *294* (1−2), 234−240.
(53) Xantheas, S. S. Cooperativity and hydrogen bonding network in water clusters. *Chem. Phys.* **2000**, *258*, 225−231.
(54) Liew, C. C.; Inomata, H.; Arai, K.; Saito, S. Three-dimensional structure and hydrogen bonding of water in sub- and supercritical regions: A molecular simulation study. *J. Supercrit. Fluids* **1998**, *13* (1−3), 83−91.
(55) Berg, R. W.; Deetlefs, M.; Seddon, K. R.; Shim, I.; Thompson, J. M. Raman and ab Initio Studies of Simple and Binary 1-Alkyl-3-methylimidazolium Ionic Liquids. *J. Phys. Chem. B* **2005**, *109* (40), 19018−19025.
(56) Chang, H.-C.; Jiang, J.-C.; Tsai, W.-C.; Chen, G.-C.; Lin, S. H. Hydrogen Bond Stabilization in 1,3-Dimethylimidazolium Methyl Sulfate and 1-Butyl-3-Methylimidazolium Hexafluorophosphate Probed by High Pressure: The Role of Charge-Enhanced C−H···O Interactions in the Room-Temperature Ionic Liquid. *J. Phys. Chem. B* **2006**, *110* (7), 3302−3307.
(57) Talaty, E. R.; Raja, S.; Storhaug, V. J.; Dölle, A.; Carper, W. R. Raman and Infrared Spectra and ab Initio Calculations of C_{2-4}MIM Imidazolium Hexafluorophosphate Ionic Liquids. *J. Phys. Chem. B* **2004**, *108* (35), 13177−13184.
(58) Steinberg, G.; Ottolenghi, M.; Sheves, M. pK_a of the protonated Schiff base of bovine rhodopsin. A study with artificial pigments. *Biophys. J.* **1993**, *64* (5), 1499−1502.
(59) Rai, G.; Kumar, A. A reversal from endothermic to exothermic behavior of imidazolium-based ionic liquids in molecular solvents. *Chem. Phys. Lett.* **2010**, *496* (1−3), 143−147.
(60) Rai, G.; Kumar, A. An enthalpic approach to delineate the interactions of cations of imidazolium-based ionic liquids with molecular solvents. *Phys. Chem. Chem. Phys.* **2011**, *13* (32), 14716−14723.
(61) Ab Rani, M. A.; Brant, A.; Crowhurst, L.; Dolan, A.; Lui, M.; Hassan, N. H.; Hallett, J. P.; Hunt, P. A.; Niedermeyer, H.; Perez-Arlandis, J. M.; Schrems, M.; Welton, T.; Wilding, R. Understanding the polarity of ionic liquids. *Phys. Chem. Chem. Phys.* **2011**, *13* (37), 16831−16840.
(62) Palomar, J.; Torrecilla, J. S.; Lemus, J.; Ferro, V. R.; Rodriguez, F. A COSMO-RS based guide to analyze/quantify the polarity of ionic liquids and their mixtures with organic cosolvents. *Phys. Chem. Chem. Phys.* **2010**, *12* (8), 1991−2000.